arXiv:hep-ph/0311275v2 9 Feb 2004

Updated analysis of meson-nucleon sigma terms in the perturbative chiral quark model

T. Inoue, V. E. Lyubovitskij, Th. Gutsche and Amand Faessler

Institut für Theoretische Physik, Universität Tübingen,
Auf der Morgenstelle 14, D-72076 Tübingen, Germany

Abstract

We present an updated analysis of meson-baryon sigma terms in the perturbative chiral quark model, which is based on effective chiral Lagrangian. The new feature concerns the inclusion of excited states in the quark propagator. Its influence on meson loops is shown to lead in particular for the pion-nucleon sigma term to an enhancement relevant for the current evaluation of this quantity. We also determine various flavor combinations of the scalar nucleon form factors and their respective low-momentum transfer limits.

I. INTRODUCTION

Meson-nucleon sigma terms provide a direct measure of the scalar quark condensates in the nucleon and thereby also constitute an indicator for the mechanism of explicit chiral symmetry breaking. Reviews on sigma-term physics including recent theoretical and experimental advances and a compilation of results can be found in Ref. [1–5].

The pion-nucleon sigma term, $\sigma_{\pi N}$, is an essential quantity for the study of low energy hadron physics. It is defined by the scalar density operator $\hat{m}(\bar{u}u + \bar{d}d)$ averaged over the nucleon or equivalently by $\sigma_{\pi N}(t = 0)$, the scalar form factor of the nucleon at zero momentum transfer squared. The canonical value of the πN sigma term $\sigma_{\pi N} = 45 \pm 8$ MeV [6] was originally extracted from a dispersional analysis of πN scattering data, while in addition exploiting the chiral symmetry constraints. In particular, the value of the sigma-term, $\sigma_{\pi N} = 45 \pm 8$ MeV, has been deduced from the analysis of two quantities: $\sigma_{\pi N}(t = 2M_\pi^2) = 60 \pm 8$ MeV, the scalar nucleon form factor at the Cheng-Dashen (CD) point $t = 2M_\pi^2$, and the difference $\Delta_\sigma = \sigma_{\pi N}(2M_\pi^2) - \sigma_{\pi N}(0) = 15.2 \pm 0.4$ MeV [6] as induced by explicit chiral symmetry breaking. The value of the scalar form factor at the CD point was close to the one based on a different extraction scheme (hyperbolic dispersion relations) from pion-nucleon scattering data: $\sigma_{\pi N}(t = 2M_\pi^2) = 64 \pm 8$ MeV [7].

An accurate analysis of the σ term in chiral perturbation theory (ChPT) [8], relating the value of σ at the CD point to the chiral limit, yields $\Delta_\sigma = 14.0$ MeV $+2M^4\bar{e}_2$; M is the pion mass in the leading order of the chiral expansion and $\bar{e}_2$ is the fourth-order renormalized low-energy constant which is supposed to be small. A recent calculation of the shift Δ_σ in

ChPT using an alternative renormalization scheme [9] gives a similar result of $\Delta_\sigma = 16.9$ MeV $+2M^4\beta$, where $\beta = \bar{e}_2$. The lattice-regularized ChPT predicts a somewhat smaller value of $\Delta_\sigma \sim 10.1 - 11$ MeV within the variation of the lattice spacing parameter [10]. Therefore, the ChPT [8] approaches confirm the original result of Ref. [6] with a consistent value for Δ_σ of about 15 MeV.

During the last few years updated analyses of also new pion-nucleon scattering data lead to a dramatic increase in the value of $\sigma_{\pi N}(2M_\pi^2)$: 88 ± 15 MeV [11], 71 ± 9 MeV [12], 79 ± 7 MeV [13]. Although there is criticism [14] on the reliability of the recent results on $\sigma_{\pi N}(2M_\pi^2)$, these new values raise the result for the empirical πN sigma term to $59 - 88$ MeV. The conclusion of Ref. [14] is that the higher values for $\sigma_{\pi N}(t = 2M_\pi^2)$, which were obtained in Refs. [11–13], can be mainly related to the πN D-wave contribution, but its usage is not consistent with analyticity.

Theoretical studies tend to predict a value for the πN sigma term, which is closer to the canonical result of $\sigma_{\pi N} = 45$ MeV. The most naive estimate based on the valence quark picture of the nucleon yields only about 15 MeV. The inclusion of the quark-antiquark sea of the nucleon is essential to enhance the basic valence quark result. Theoretical models which somehow take the sea into account therefore give a larger reasonable size of the sigma term. For a detailed discussion of the theoretical results for $\sigma_{\pi N}$ see Ref. [5]. Closely linked to the problem of the pion-nucleon sigma-term are other related quantities like the kaon-nucleon sigma terms and the strangeness content of the nucleon.

In a previous paper [15] we performed a detailed analysis of meson-nucleon sigma-terms in the context of the perturbative chiral quark model (PCQM) [15–21]. The PCQM is based on the non-linear σ-model quark-meson Lagrangian and includes a phenomenological confinement potential. Baryons are considered as bound states of valence quarks surrounded by a cloud of pseudoscalar mesons as imposed by chiral symmetry requirements. This model was successfully applied to the electromagnetic properties of the nucleon [16,17], πN scattering including radiative corrections [18], double β-decay processes [19], the strange nucleon form factors [20] and the nucleon axial vector coupling constant and form-factor [21].

In Ref. [15] we reproduced the conventional value of $\sigma_{\pi N} = 45 \pm 5$ MeV which is mostly explained by the pion cloud. We showed that the valence quarks give a contribution of 13 MeV, while terms due to the kaon and η-meson cloud are sufficiently suppressed. All calculations for loop diagrams were performed with a quark propagator where only the ground state contribution, corresponding to hadronic nucleon and delta intermediate states, was taken into account.

In the current work, we update our analysis of meson-nucleon sigma-terms and include a discussion of the scalar nucleon form factors. As a new feature we investigate the saturation effects of the quark propagator by low-lying excited states. In particular, we find that the inclusion of excited states leads to an increase of the $\sigma_{\pi N}$ term from ~ 45 MeV to ~ 55 MeV. Additionally, we present the calculation of quantities which are not discussed in Ref. [15], like the scalar pion- and kaon-nucleon form factors and their respective slopes, and the value of $\sigma_{\pi N}(2M_\pi^2)$.

In the present paper we proceed as follows. In Sect.II we review the basic notions of the PCQM. In Sec.III we present the calculation of the scalar nucleon form factors $\sigma_{\pi N}(Q^2)$ and $\sigma_{KN}(Q^2)$. We discuss their radii, the value $\sigma_{\pi N}(Q^2)$ at the Cheng-Dashen point and at zero recoil (sigma-terms). We also give a set of predictions for related quantities: the non-strange and strange quark condensates, the strangeness content of the nucleon, the isovector KN sigma-term $\sigma_{KN}^{I=1}$ and others. Sec.IV contains a summary of our conclusions.

II. THE PERTURBATIVE CHIRAL QUARK MODEL (PCQM)

The perturbative chiral quark model [15–20] is based on an effective chiral Lagrangian describing the valence quarks of baryons as relativistic fermions moving in an external field (static potential) $V_{\rm eff}(r) = S(r) + \gamma^0 V(r)$ with $r = |\vec{x}|$ [15,16], which in the SU(3)-flavor version are supplemented by a cloud of Goldstone bosons (π, K, η):

$$\begin{aligned}\mathcal{L}_\chi(x) &= \bar{\psi}(x)\,[i\,\partial\!\!\!/ \,-\,\gamma^0 V(r)]\,\psi(x) \,+\, \frac{F^2}{4}\,{\rm Tr}[\partial^\mu U(x)\,\partial^\mu U^\dagger(x)] \\ &- \bar{\psi}(x)\,S(r)\left[\frac{U(x)\,+U^\dagger(x)}{2} \,+\, \gamma^5\,\frac{U(x)\,-\,U^\dagger(x)}{2}\right]\psi(x)\end{aligned} \tag{1}$$

where $U(x)$ is the chiral field and $F = 88$ MeV is the pion decay constant in the chiral limit [22]. We define the chiral field using the exponentional parametrization $U = \exp[i\hat{\Phi}/F]$ where $\hat{\Phi} = \sum\limits_{i=1}^{8} \Phi_i \lambda_i = \sum\limits_{P} \Phi_P \lambda_P$ is the octet matrix of pseudoscalar mesons with $P = \pi^\pm, \pi^0, K^\pm, K^0, \bar{K}^0, \eta$. The relations between the sets $\{\Phi_P, \lambda_P\}$ and $\{\Phi_i, \lambda_i\}$ are given in the Appendix.

Treating Goldstone fields as small fluctuations around the three-quark (3q) core we have the linearized effective Lagrangian[1]:

$$\begin{aligned}\mathcal{L}_{\rm eff}(x) &= \bar{\psi}(x)[i\,\partial\!\!\!/ - S(r) - \gamma^0 V(r)]\psi(x) + \frac{1}{2}\sum_{i=1}^{8}[\partial_\mu \Phi_i(x)]^2 \\ &- \bar{\psi}(x) S(r) i\gamma^5 \frac{\hat{\Phi}(x)}{F}\psi(x) + \mathcal{L}_{\chi SB}(x).\end{aligned} \tag{2}$$

In Eq. (2) we include the term $\mathcal{L}_{\chi SB}$ which contains the mass contributions both for quarks and mesons and explicitly breaks chiral symmetry:

$$\mathcal{L}_{\chi SB}(x) = -\bar{\psi}(x)\mathcal{M}\psi(x) - \frac{B}{2}{\rm Tr}[\hat{\Phi}^2(x)\mathcal{M}]\,. \tag{3}$$

Here, $\mathcal{M} = {\rm diag}\{m_u, m_d, m_s\}$ is the mass matrix of current quarks and $B = -\langle 0|\bar{u}u|0\rangle/F^2$ is the quark condensate constant. In the numerical calculations we restrict to the isospin symmetry limit $m_u = m_d = \hat{m}$. After diagonalization the meson mass term takes the form

$$\frac{B}{2}\,{\rm Tr}[\hat{\Phi}^2(x)\mathcal{M}] = \frac{1}{2}\sum_P\, M_P^2\, \Phi_P^2(x) \tag{4}$$

where M_P is the set of masses of the pseudoscalar mesons. We rely on the standard picture of chiral symmetry breaking [23] and for the masses of pseudoscalar mesons we use the leading term in their chiral expansion, i.e. linear in the current quark masses (see, Eq.(A4) in the Appendix). In the isospin limit they are given by

---

[1] In Eq. (A5) of the Appendix the linearized Lagrangian is given in the basis of $\{\Phi_P, \lambda_P\}$.

$$M_\pi^2 = 2\hat{m}B, \quad M_K^2 = (\hat{m} + m_s)B, \quad M_\eta^2 = \frac{2}{3}(\hat{m} + 2m_s)B. \tag{5}$$

The following set of parameters [23] is chosen in our evaluation

$$\hat{m} = 7 \text{ MeV}, \ \frac{m_s}{\hat{m}} = 25, \ B = \frac{M_{\pi^+}^2}{2\hat{m}} = 1.4 \text{ GeV}. \tag{6}$$

Meson masses obtained in Eq. (5) satisfy the Gell-Mann-Oakes-Renner and the Gell-Mann-Okubo relation. In addition, the linearized effective Lagrangian in Eq. (2) fulfils the PCAC requirement.

We expand the quark field ψ in the basis of potential eigenstates as

$$\psi(x) = \sum_\alpha b_\alpha u_\alpha(\vec{x}) \exp(-i\mathcal{E}_\alpha t) + \sum_\beta d_\beta^\dagger v_\beta(\vec{x}) \exp(i\mathcal{E}_\beta t)\,, \tag{7}$$

where the sets of quark $\{u_\alpha\}$ and antiquark $\{v_\beta\}$ wave functions in orbits α and β are solutions of the Dirac equation with the static potential $V_{\rm eff}(r)$. The expansion coefficients b_α and $d_\beta^\dagger$ are the corresponding single quark annihilation and antiquark creation operators.

We formulate perturbation theory in the expansion parameter $\hat{\Phi}(x)/F \sim 1/\sqrt{N_c}$ and treat finite current quark masses perturbatively [16]. The expansion in powers of $\hat{\Phi}(x)/F$ corresponds to an expansion of matrix elements, formulated in momentum space, in powers of p/F where p is the three-momentum of the meson field. All calculations are performed at one loop or at order of accuracy $o(1/F^2, \hat{m}, m_s)$. In the calculation of matrix elements we project quark diagrams on the respective baryon states. The baryon states are conventionally set up by the product of the SU(6) spin-flavor and SU(3)$_{\rm c}$ color wave functions, where the nonrelativistic single quark spin wave function is replaced by the relativistic solution $u_\alpha(\vec{x})$ of the Dirac equation

$$\left[-i\gamma^0\vec{\gamma}\cdot\vec{\nabla} + \gamma^0 S(r) + V(r) - \mathcal{E}_\alpha\right] u_\alpha(\vec{x}) = 0, \tag{8}$$

where $\mathcal{E}_\alpha$ is the single-quark energy. For the description of baryon properties we use the effective potential $V_{\rm eff}(r)$ with a quadratic radial dependence [15,16]:

$$S(r) = M_1 + c_1 r^2, \qquad V(r) = M_2 + c_2 r^2 \tag{9}$$

with the particular choice

$$M_1 = \frac{1 \, - \, 3\rho^2}{2\,\rho R}, \qquad M_2 = \mathcal{E}_0 - \frac{1 \, + \, 3\rho^2}{2\,\rho R}, \qquad c_1 \equiv c_2 = \frac{\rho}{2R^3}. \tag{10}$$

Here, $\mathcal{E}_0$ is the single-quark ground-state energy; R are ρ are parameters related to the ground-state quark wave function u_0:

$$u_0(\vec{x}) \; = \; N \, \exp\left[-\frac{\vec{x}^{\,2}}{2R^2}\right] \begin{pmatrix} 1 \\ i\rho\,\vec{\sigma}\vec{x}/R \end{pmatrix} \chi_s\,\chi_f\,\chi_c, \tag{11}$$

where $N = [\pi^{3/2} R^3 (1+3\rho^2/2)]^{-1/2}$ is a normalization constant; χ_s, χ_f, χ_c are the spin, flavor and color quark wave function, respectively. The constant part of the scalar potential M_1 can be interpreted as the constituent mass of the quark, which is simply the displacement of the current quark mass due to the potential $S(r)$. The parameter ρ is related to the axial charge g_A of the nucleon calculated in zeroth-order (or 3q-core) approximation:

$$g_A = \frac{5}{3}\Big(1 - \frac{2\rho^2}{1+\frac{3}{2}\rho^2}\Big) = \frac{5}{3}\Big(1 - \frac{2}{3}(1-\gamma)\Big) \tag{12}$$

where

$$\gamma = \frac{1-\frac{3}{2}\rho^2}{1+\frac{3}{2}\rho^2} \tag{13}$$

is the relativistic reduction factor (the specific value $\gamma = 1$ corresponds to the nonrelativistic limit). Therefore, ρ can be replaced by g_A using the matching condition (12). The parameter R is related to the charge radius of the proton in the zeroth-order approximation as

$$\langle r^2_E \rangle^P_{LO} = \int d^3x \, u_0^\dagger(\vec{x}) \, \vec{x}^{\,2} \, u_0(\vec{x}) \; = \; \frac{3R^2}{2} \, \frac{1 \, + \, \frac{5}{2}\,\rho^2}{1 \, + \, \frac{3}{2}\,\rho^2}. \tag{14}$$

In our calculations we use the value g_A=1.25 [15,16]. With ρ fixed, we have only one free parameter, that is R. In the numerical studies R is varied in the region from 0.55 fm to 0.65 fm, which corresponds to a change of $\langle r^2_E \rangle^P_{LO}$ from 0.5 to 0.7 fm^2. In the current work we use the central value of $R = 0.6$ fm.

The expectation value of an operator $\hat{A}$ is set up as:

$$\langle \hat{A} \rangle = {}^B\langle \phi_0 | \sum_{n=0}^{\infty} \frac{i^n}{n!} \int d^4x_1 \ldots \int d^4x_n T[\mathcal{L}_I(x_1) \ldots \mathcal{L}_I(x_n) \hat{A}] | \phi_0 \rangle^B_c, \tag{15}$$

where the state vector $|\phi_0\rangle$ corresponds to the unperturbed three-quark state ($3q$-core). Superscript "B" in (15) indicates that the matrix elements have to be projected onto the respective baryon states, whereas subscript "c" refers to contributions from connected graph only. $\mathcal{L}_I(x)$ of Eq. (15) refers to the linearized quark-meson interaction Lagrangian:

$$\mathcal{L}_I(x) = -\bar{\psi}(x) i\gamma^5 \frac{\hat{\Phi}(x)}{F} S(r) \psi(x). \tag{16}$$

For the evaluation of Eq.(15) we apply Wick's theorem with the appropriate propagators for quarks and mesons.

For the quark field we use a Feynman propagator for a fermion in a binding potential with:

$$\begin{aligned} iG_\psi(x,y) &= \langle 0 | T\{\psi(x)\bar{\psi}(y)\} | 0 \rangle \\ &= \theta(x_0 - y_0) \sum_\alpha u_\alpha(\vec{x}) \bar{u}_\alpha(\vec{y}) e^{-i\mathcal{E}_\alpha (x_0 - y_0)} - \theta(y_0 - x_0) \sum_\beta v_\beta(\vec{x}) \bar{v}_\beta(\vec{y}) e^{i\mathcal{E}_\beta (x_0 - y_0)}. \end{aligned} \tag{17}$$

In previous applications [15,16,18–20] we restricted the expansion of the quark propagator to its ground state with:

$$iG_\psi(x,y) \to iG_0(x,y) \doteq u_0(\vec{x})\,\bar{u}_0(\vec{y})\,e^{-i\mathcal{E}_0(x_0-y_0)}\,\theta(x_0-y_0). \tag{18}$$

Such a truncation can be considered as an additional regularization of the quark propagator, where in the case of SU(2)-flavor intermediate baryon states in loop-diagrams are restricted to N and Δ. We recently updated our approach by including excited quark states in the propagator of Eq. (17) and analyzed their influence on the matrix elements for the N-Δ transitions considered [17]. Following set of excited quark states are included: the first p-states ($1p_{1/2}$ and $1p_{3/2}$ in the non-relativistic notation) and the second excited states ($1d_{3/2}, 1d_{5/2}$ and $2s_{1/2}$). For the given form of the effective potential (9) the Dirac equation can be solved analytically. The corresponding expressions for the wave functions of the excited quark states are given in the Appendix of Ref. [17]. In the current work we also include the effects of the excited states in the quark propagator following the original work of Ref. [17].

For the meson fields we adopt the free Feynman propagator with

$$i\Delta_{PP'}(x-y) = \langle 0|T\{\Phi_P(x)\Phi_{P'}(y)\}|0\rangle = \delta_{PP'}\int\frac{d^4k}{(2\pi)^4 i}\frac{\exp[-ik(x-y)]}{M_P^2-k^2-i\epsilon}. \tag{19}$$

III. MESON-NUCLEON SIGMA TERMS IN THE PCQM

The scalar density operators S_i^{PCQM} ($i=u,d,s$), relevant for the calculation of the meson-baryon sigma-terms in the PCQM, are defined as the partial derivatives of the model χSB Hamiltonian $\mathcal{H}_{\chi SB} = -\mathcal{L}_{\chi SB}$ at $m_u \neq m_d$ with respect to the current quark mass of i-th flavor m_i. After taking the derivative we apply the isospin limit with $m_u = m_d = \hat{m}$. Here we obtain

$$S_i^{PCQM} \doteq \frac{\partial\mathcal{H}_{\chi SB}}{\partial m_i} = S_i^{val} + S_i^{sea}, \tag{20}$$

where S_i^{val} is the set of valence-quark operators coinciding with the ones obtained from the QCD Hamiltonian

$$S_u^{val} = \bar{u}u, \qquad S_d^{val} = \bar{d}d, \qquad S_s^{val} = \bar{s}s. \tag{21}$$

The set of sea-quark operators S_i^{sea} arises from the pseudoscalar meson mass term:

$$\begin{aligned} S_u^{sea} &= B\left\{\pi^+\pi^- + \frac{\pi^0\pi^0}{2} + K^+K^- + \frac{\eta^2}{6}\right\}, \\ S_d^{sea} &= B\left\{\pi^+\pi^- + \frac{\pi^0\pi^0}{2} + K^0\bar{K}^0 + \frac{\eta^2}{6}\right\}, \\ S_s^{sea} &= B\left\{K^+K^- + K^0\bar{K}^0 + \frac{2}{3}\eta^2\right\}. \end{aligned} \tag{22}$$

We calculate the scalar nucleon form factors and meson-baryon sigma-terms using Eq. (15) in the isospin limit ($m_u = m_d = \hat{m}$) and at order of accuracy $o(1/F^2, \hat{m}, m_s)$. For technical details concerning the perturbative analysis of Eq. (15) see Refs. [15,16]. For example, the expression for the scalar form factor $\sigma_{\pi N}(Q^2)$ is given as

$$\sigma_{\pi N}(Q^2) = \hat{m} \; {}^p\langle\phi_0| \sum_{n=0}^{2} \frac{i^n}{n!} \int \delta(t)\, d^4x\, d^4x_1 \, \ldots \, d^4x_n \, e^{-iqx} \times T[\mathcal{L}_I(x_1) \ldots \mathcal{L}_I(x_n)\, S_{u+d}^{PCQM}(x)\,]|\phi_0\rangle_c^p \tag{23}$$

where we introduced the shorted notation

$$S_{q\pm q'}^{PCQM} = S_q^{PCQM} \pm S_{q'}^{PCQM} \,. \tag{24}$$

As in previous work, for example in the calculation of electromagnetic nucleon form factors [16], we restrict our kinematics to a specific frame, that is the Breit frame. This constraint is sufficient to guarantee local gauge invariance concerning the coupling of the electromagnetic field (for a detailed discussion see Ref. [16]). The Breit frame is specified as follows: the initial momentum of the nucleon is $p = (E, -\vec{q}/2)$, the final momentum is $p' = (E, \vec{q}/2)$ and the 4-momentum of the external field is $q = (0, \vec{q}\,)$ with $p' = p + q$. The space-like momentum transfer squared is given by $Q^2 = -q^2 = \vec{q}^{\,2}$.

The following diagrams contribute to the scalar nucleon form factors (and therefore the sigma-terms) up to the one-loop level: tree level diagram (Fig.1a) with the insertion of the valence-quark scalar density S_i^{val} into the quark line, the meson cloud (Fig.1b) and meson exchange diagrams (Fig.1c) with insertion of the sea-quark scalar density S_i^{sea} to the meson line. We do not take into account the diagram generated by dressing of the valence-quark scalar density operator by the meson field since it is proportional to $\hat{m}/F^2$ or m_s/F^2 and, therefore, contributes only to the next order of our perturbation expansion.

The πN sigma term $\sigma_{\pi N} = \sigma_{\pi N}(0)$ is then obtained as

$$\sigma_{\pi N} \, = \, \sigma_{\pi N}^{val} \, + \, \sigma_{\pi N}^{sea} \tag{25}$$

where

$$\sigma_{\pi N}^{val} \, = \, 3\gamma\hat{m} \tag{26}$$

is due to the valence quarks and

$$\sigma_{\pi N}^{sea} = \sum_{\Phi=\pi,K,\eta} \sigma_{\pi N}^{\Phi} = \sum_{\Phi=\pi,K,\eta} d_N^{\Phi\,(1)}\, \Gamma_\Phi^{(1)} \; + \sum_{\Phi=\pi,K,\eta} d_N^{\Phi\,(2)}\, \Gamma_\Phi^{(2)} \tag{27}$$

is the sea-quark contribution. Here, $d_N^{\Phi\,(i)}$ with $\Phi = \pi, K$ or η are the recoupling coefficients defining the partial contributions of the π, K, and η-meson cloud related to the diagrams of Fig.1b (with $i = 1$) and Fig.1c (with $i = 2$):

$$\begin{aligned} d_N^{\pi\,(1)} &= \frac{81}{400}, \qquad d_N^{K\,(1)} = \frac{54}{400}, \qquad d_N^{\eta\,(1)} = \frac{9}{400}, \\ d_N^{\pi\,(2)} &= \frac{90}{400}, \qquad d_N^{K\,(2)} \equiv 0, \qquad\;\; d_N^{\eta\,(2)} = -\frac{6}{400}\,. \end{aligned} \tag{28}$$

Analytical expressions for the vertex functions $\Gamma_\Phi^{(1)}$ and $\Gamma_\Phi^{(2)}$, when the quark propagator is truncated to the ground state, are given in Ref. [15]. The additional contribution of excited quark states are evaluated as laid out in Ref. [17]. Note that the Feynman-Hellmann (FH) theorem, relating the pion-nucleon sigma-term $\sigma_{\pi N}$ to the nucleon mass m_N

$$\sigma_{\pi N} = \hat{m}\frac{\partial m_N}{\partial \hat{m}}. \tag{29}$$

is fulfiled in the present model calculation for any form of the quark propagator (truncated to the ground state or with inclusion of excited states) as originally proven in Ref. [15]. The nucleon mass in our approach is given by

$$m_N = 3\mathcal{E}_0 + 3\gamma\hat{m} \ + \Pi_N \tag{30}$$

where Π_N is the self-energy operator encoding the nucleon mass shift due to the meson cloud. Two diagrams contribute to Π_N at one loop: the meson cloud (Fig.2a) and the meson exchange diagram (Fig.2b):

$$\Pi_N \ = \sum_{\Phi=\pi,K,\eta} d_N^{\Phi\,(1)}\,\Pi_\Phi^{(1)} \ + \sum_{\Phi=\pi,K,\eta} d_N^{\Phi\,(2)}\,\Pi_\Phi^{(2)} \tag{31}$$

where $\Pi_\Phi^{(1)}$ and $\Pi_\Phi^{(2)}$ are the self-energies corresponding to the diagrams of Fig.2a and Fig.2b, respectively. In accordance with the FH theorem (29), the vertex functions $\Gamma_\Phi^{(i)}$ are related to the partial derivative of the self-energies $\Pi_\Phi^{(i)}$ with respect to $\hat{m}$:

$$\Gamma_\Phi^{(i)} \ = \ \hat{m}\,\frac{\partial}{\partial\hat{m}}\,\Pi_\Phi^{(i)}\,. \tag{32}$$

The recoupling coefficients $d_N^{\Phi\,(i)}$ of Eq. (31), defining the partial contributions of the π, K, and η-meson cloud to the energy shift of the nucleon, are therefore the same as in Eq. (27).

We also consider quantities which partially incorporate information about the strangeness content of the nucleon: the strangeness y_N, the kaon-nucleon sigma-terms $\sigma_{KN}^u \equiv \sigma_{KN}^{(1)}$, σ_{KN}^d, $\sigma_{KN}^{(2)}$, $\sigma_{KN}^{I=0}$ and $\sigma_{KN}^{I=1}$, the eta-nucleon sigma-term $\sigma_{\eta N}$ and the respective scalar form factors $\sigma_{KN}^u(Q^2) \equiv \sigma_{KN}^{(1)}(Q^2)$, $\sigma_{KN}^d(Q^2)$, $\sigma_{KN}^{(2)}(Q^2)$, $\sigma_{KN}^{I=0}(Q^2)$, $\sigma_{KN}^{I=1}(Q^2)$ and $\sigma_{\eta N}(Q^2)$ (in particular their slopes). These quantities of interest are defined by the standard formulas:

$$\begin{aligned}
\sigma_{KN}^u &\equiv \sigma_{KN}^{(1)} = \frac{\hat{m}+m_s}{2}\langle p|S_{u+s}^{PCQM}|p\rangle\,,\\
\sigma_{KN}^d &= \frac{\hat{m}+m_s}{2}\langle p|S_{d+s}^{PCQM}|p\rangle\,,\\
\sigma_{KN}^{(2)} &\equiv 2\sigma_{KN}^{(d)} - \sigma_{KN}^{(u)} = \frac{\hat{m}+m_s}{2}\langle p|2\,S_{d+s}^{PCQM} - S_{u+s}^{PCQM}|p\rangle\,,\\
\sigma_{KN}^{I=0} &= \frac{\sigma_{KN}^u + \sigma_{KN}^d}{2} = \frac{\hat{m}+m_s}{4}\langle p|S_{u+s}^{PCQM} \ + \ S_{d+s}^{PCQM}|p\rangle\,,\\
\sigma_{KN}^{I=1} &= \frac{\sigma_{KN}^u - \sigma_{KN}^d}{2} = \frac{\hat{m}+m_s}{4}\langle p|S_{u-d}^{PCQM}|p\rangle\,,\\
\sigma_{\eta N} &= \frac{1}{3}\langle p|\hat{m}\,S_{u+d}^{PCQM} \ + \ 4\,m_s\,S_s^{PCQM}|p\rangle\,,\\
F_S &= \frac{1}{2}\,\langle p|S_{u-s}^{PCQM}|p\rangle\,,\\
D_S &= \frac{1}{2}\,\langle p|S_{u-d}^{PCQM} \ - \ S_{d-s}^{PCQM}|p\rangle\,,\\
y_N &= 2\,\frac{\langle p|S_s^{PCQM}|p\rangle}{\langle p|S_{u+d}^{PCQM}|p\rangle}\,,
\end{aligned} \tag{33}$$

where $|p\rangle$ denotes a one-proton state normalized to unity $\langle p|p\rangle = 1$. The generic matrix element $\langle p|S_q^{PCQM}|p\rangle$ is again set up by the expression

$$\langle p|S_q^{PCQM}|p\rangle \doteq {}^p\langle\phi_0|\sum_{n=0}^{2}\frac{i^n}{n!}\int d^3x\, d^4x_1 \,\ldots\, d^4x_n\; T[\mathcal{L}_I(x_1)\ldots\mathcal{L}_I(x_n)\, S_q^{PCQM}(\vec{x})\,]|\phi_0\rangle_c^p\,. \qquad (34)$$

The scalar nucleon form factors and their respective slopes are defined in analogy with Eqs. (23) and (36), where latter equation will be set up in the forthcoming section.

IV. RESULTS

We first discuss the results for the scalar nucleon form factor $\sigma_{\pi N}(Q^2)$ and the corresponding πN sigma-term. In Ref. [15] we calculated the $\sigma_{\pi N}$ sigma-term with the quark propagator restricted to the ground state. The result we obtained there was 45 ± 5 MeV, where the variation of the value is due to a change of the range parameter R. For the central value of $R = 0.6$ fm we obtain $\sigma_{\pi N} = 42.5$ MeV, where the valence-quark contribution is $\sigma_{\pi N}^{val} = 13.1$ MeV (i.e. 1/3 of the total value) and the meson-cloud contribution is dominated by the pions with $\sigma_{\pi N}^{sea} = 29.4$ MeV (i.e. 2/3 of total value).

Inclusion of the excited quark states obviously does not change the result for $\sigma_{\pi N}^{val}$ but leads to an increase for $\sigma_{\pi N}^{sea}$ from 29.4 MeV to 41.6 MeV. Hence, we obtain a sizable increase of the sigma term by about 12 MeV leading to the final value of $\sigma_{\pi N} = 54.7$ MeV. Again, the main contribution is due to pion loops, whereas kaon and eta loops are strongly suppressed. The obtained value of 54.7 MeV is still comparable to the upper limit of the canonical result 45 ± 8 MeV obtained in Ref. [6]. It is also in agreement with the result obtained in the framework of relativistic baryon ChPT up to next-next-to-leading order (NNLO) based on an extrapolation of this observable from two-flavor lattice QCD results: $\sigma_{\pi N} = 53 \pm 8$ MeV at the physical value of the pion mass [24]. For a more detailed comparison to other theoretical approaches we relegate to the recent paper [5].

Our final results are compiled as:

$$\begin{aligned} &\sigma_{\pi N} = 54.7\ \text{MeV}, \quad &&\sigma_{\pi N}^{val} = 13.1\ \text{MeV}, \quad &&\sigma_{\pi N}^{sea} = 41.6\ \text{MeV}, \\ &\sigma_{\pi N}^{\pi} = 39.4\ \text{MeV}, \quad &&\sigma_{\pi N}^{K} = 2.1\ \text{MeV}, \quad &&\sigma_{\pi N}^{\eta} = 0.1\ \text{MeV}\,, \end{aligned} \qquad (35)$$

where the explicit meson loop contributions are made explicit in the last line.

In Fig.3 we plot the behavior of the scalar nucleon form factor $\sigma_{\pi N}(Q^2)$ in the space-like region up to 0.5 GeV^2. The partial contributions of the valence quarks and the meson cloud are indicated separately. The meson cloud dominates the scalar nucleon form factor for small $Q^2 < 0.15$ GeV^2, while the valence quarks contribute mostly at large $Q^2 > 0.3$ GeV^2. The limiting value for $\sigma_{\pi N}(Q^2)$ at $Q^2 = 0$ is nothing but the πN sigma-term as discussed above. The slope of the scalar nucleon form factor is defined by the standard formula:

$$\langle r^2\rangle_N^S \doteq \langle r^2\rangle_{\pi N}^S = -\frac{6}{\sigma_{\pi N}(0)}\frac{d\sigma_{\pi N}(Q^2)}{dQ^2}\bigg|_{Q^2\,=\,0}\,. \qquad (36)$$

Our result is

$$\langle r^2\rangle^S_N = 1.5 \text{ fm}^2 \tag{37}$$

which is comparable to the model-independent prediction of Ref. [6]: $\langle r^2\rangle^S_N \simeq 1.6$ fm^2. As pointed out in Ref. [6], the result for the range of the scalar form factor is larger than the charge radius of nucleon associated with the isovector form factor since "the scalar current $\bar{u}u + \bar{d}d$ is much more sensitive to the pion halo surrounding the nucleon than the electromagnetic current". In Fig.4 we compare our prediction for the scalar form factor $\sigma_{\pi N}(Q^2)$ to results of other theoretical calculations: lattice QCD [25], soliton models (NJL-soliton model [26] and chiral quark soliton model [5]) and the relativistic baryon chiral perturbation theory [9]. The lattice result for $\sigma_{\pi N}(Q^2)$ [25] with $\sigma_{\pi N}(0) = 49.7 \pm 2.6$ MeV decreases slower than ours. Their prediction for the slope $\sqrt{\langle r^2\rangle^S_N} = 0.85(4)$ fm is also smaller than our estimate and the model-independent results of Ref. [6]. The form factor $\sigma_{\pi N}(Q^2)$ calculated in Ref. [26] starts from 40.8 MeV at zero recoil, crosses our form factor at around 0.17 GeV^2 and decreases slower than our curve. The result for $\langle r^2\rangle^S_N = 1.5$ fm^2 coincides with ours. The result of Ref. [5] has the same shape but is shifted in average by about $\sim$ 15 MeV upward with respect to our result. The corresponding values of $\sigma_{\pi N}(0)$ and $\langle r^2\rangle^S_N$ are 67.9 MeV and 1 fm^2. The scalar form factor calculated in Ref. [9] is smaller than ours in magnitude in the Euclidean region and decreases very quickly. It vanishes at 0.2 GeV. The value of $\sigma_{\pi N}(0) = 40.5$ MeV calculated by neglecting higher-order corrections is close to the canonical value of $\sigma_{\pi N}(0) = 45 \pm 8$ MeV [6].

Next we extrapolate the scalar nucleon form factor to the time-like region $t = -Q^2$ for small t by using the linear approximation:

$$\sigma_{\pi N}(t) \, = \, \sigma_{\pi N}(0) \left(1 \, + \, \frac{1}{6} \, \langle r^2\rangle^S_N \, \cdot \, t \, + \, O(t^2) \right). \tag{38}$$

With Eqs. (38) and (36) we obtain for the difference

$$\Delta_\sigma = \sigma_{\pi N}(2M_\pi^2) - \sigma_{\pi N}(0) = 13.8 \text{ MeV} \tag{39}$$

which is comparable to the canonical value of $\Delta_\sigma = 15.2 \pm 0.4$ MeV deduced by dispersion-relation techniques [6] and to the results obtained in ChPT: $\Delta_\sigma = 14.0$ MeV $+2M^4\bar{e}_2$ [8] and $\Delta_\sigma = 16.9$ MeV $+2M^4\beta$ [9]. The value of the $\sigma_{\pi N}(t)$ at the CD point

$$\sigma_{\pi N}(2M_\pi^2) = 68.5 \text{ MeV} \tag{40}$$

is comparable to the upper limit (68 MeV) of the value deduced in Ref. [6], close to the central value (64 MeV) extracted from the analysis of pion-nucleon scattering data [7] and smaller than the central values of the recent analyses [11–13]. Our result for Δ_σ is close to the prediction of soliton models 14.7 MeV [5] and 18.18 MeV [26]. The result of lattice QCD with $\Delta_\sigma = 6.6 \pm 0.6$ MeV is smaller than our estimate and previous results including the canonical value of Ref. [6].

Our complete results for the static nucleon properties associated with the scalar density condensates of all three flavors are summarized in Table I. There we indicate explicitly the partial contributions of the valence quarks and the meson cloud: pion, kaon and eta-meson contribution. Table I also contains the sigma-terms related to the strangeness content of the nucleon. Our result for the isosinglet KN sigma-term $\sigma^{I=0}_{KN} = 386.3$ MeV is in rather good agreement with other theoretical predictions: 389(14) MeV [25] (lattice QCD), $2.83 M_\pi = 395$ MeV [27] (chiral analysis of KN scattering). The prediction for the $\sigma^{(1)}_{KN}$ sigma-term of 419.2 MeV is close to the the result of the lattice-regularized ChPT [10]: 300-400 MeV, where the lattice space parameter is varied from ~ 1 GeV to 10 GeV. Our results for the sigma-terms $\sigma^{(1)}_{KN}$ and $\sigma^{(2)}_{KN} = 287.6$ MeV are comparable to the prediction of heavy baryon ChPT [28] (decuplet states included in the fit): $\sigma^{(1)}_{KN} = 380 \pm 40$ MeV and $\sigma^{(2)}_{KN} = 250 \pm 30$ MeV. Our result for the strangeness content of the nucleon of $y_N = 0.09$ is still smaller than the result of Ref. [6]: $y_N = 0.2$.

In the following we focus on the discussion of the isovector sigma-term $\sigma^{I=1}_{KN}$. In this case the relevant scalar density operator is given by

$$S^{\rm PCQM}_{u-d} \, = \, \bar u u - \bar d d \, + \, B \biggl\{ K^+ K^- \, - \, K^0 \bar K^0 \biggr\} \,, \tag{41}$$

where the first two terms correspond to the valence quarks. The next two terms indicate the isovector combination of the kaon with $K^+K^- - K^0\bar K^0$. The value we obtain for this sigma term is

$$\sigma^{I=1}_{KN} = 28.4 \ ({\rm Val}) + 4.5 \ ({\rm kaon\,cloud}) = 32.9 \ {\rm MeV} \,. \tag{42}$$

Our result for the isovector kaon-nucleon sigma-term is smaller than the phenomenological value ~ 50 MeV derived in Ref. [4] using the baryon mass formulas:

$$\sigma^{I=1}_{KN} \sim \frac{m_s + \hat m}{m_s - \hat m} \, \frac{m_\Xi^2 - m_\Sigma^2}{8 m_P} = 48 \ {\rm MeV} \sim 50 \ {\rm MeV} \,. \tag{43}$$

Note, the pion cloud does not contribute to $\sigma^{I=1}_{KN}$ (42), since a two-pion configuration with orbital momentum $L = 0$ only occurs with the isospin combination $I = 0$ or $I = 2$. Because of the absence of pion loop contributions $\sigma^{I=1}_{KN}$ is rather small when compared to other KN sigma-terms.

In Figs.5-10 we plot the behavior of the scalar nucleon form factors $\sigma^u_{KN}(Q^2)$, $\sigma^d_{KN}(Q^2)$, $\sigma^{(2)}_{KN}(Q^2)$, $\sigma^{I=0}_{KN}(Q^2)$, $\sigma^{I=1}_{KN}(Q^2)$ and $\sigma_{\eta N}(Q^2)$ in the space-like region up to 0.5 GeV^2. As was the case for the $\sigma_{\pi N}(Q^2)$ form factor, here we also indicate the partial contributions of the valence quarks and the meson cloud. The set of scalar nucleon form factors can be separated into three groups. The first group includes the form factors $\sigma_{\pi N}(Q^2)$, $\sigma^u_{KN}(Q^2)$, $\sigma^d_{KN}(Q^2)$, $\sigma^{I=0}_{KN}(Q^2)$, which is characterized by the dominance of the meson cloud contribution for small $Q^2 < 0.15$ GeV^2 and of the valence quarks for large $Q^2 > 0.3$ GeV^2. The second group includes the $\sigma^{I=1}_{KN}(Q^2)$ form factor which is dominated by the valence quark contribution in the whole Q^2 region. Finally, the third group includes the form factors $\sigma^{(2)}_{KN}(Q^2)$ and $\sigma_{\eta N}(Q^2)$ which are dominated by the meson cloud contribution.

For completeness, we also determined the slopes of these form factors using:

$$\langle r^2 \rangle^S_{MN} \, = \, - \, \frac{6}{\sigma_{MN}(0)} \frac{d\sigma_{MN}(Q^2)}{dQ^2} \biggr|_{Q^2\,=\,0} \,, \tag{44}$$

where our results are also given in Table I. Unfortunately, the model cannot be applied to the calculation of the σ^u_{KN} form factor at the CD point with $t = -Q^2 = 2M_K^2$ since it is kinematically far from zero recoil. This quantity is relevant for the ongoing DEAR experiment [29].

V. CONCLUSIONS

We have updated our analysis of the meson-nucleon sigma-terms applying the perturbative chiral quark model which is based on an effective chiral Lagrangian. As a new feature we include excited states in the quark propagator, which, in the context of loop diagrams, can play an important role to enhance the considered quantities. We presented a comprehensive calculation for various flavor combinations of the scalar nucleon form factors and the respective low-energy properties such as slopes and sigma terms.

In particular we showed that inclusion of excited states leads to an increase of the πN sigma term from $\sim$ 45 MeV to $\sim$ 55 MeV. The main contribution to this quantity arises from the pion cloud. We also determined the scalar nucleon form factor $\sigma_{\pi N}(Q^2)$ in the space-like region up to 0.5 GeV^2 and extrapolates it to the Cheng-Dashen point $t = -Q^2 = 2M_\pi^2$. Our result for the difference $\Delta_\sigma = \sigma_{\pi N}(2M_\pi^2) - \sigma_{\pi N}(0) = 13.8$ MeV is in good agreement with the canonical value 15.2 ± 0.4 MeV [6] and the results obtained in ChPT [8,9].

We also presented a detailed analysis of quantities related to the strangeness content of the nucleon such as KN and ηN sigma terms, y_N, KN and ηN scalar form factors and their respective slopes. To gain a deeper understanding of the various meson-nucleon sigma terms, further efforts are needed both from theoretical and experimental side.

Acknowledgments

This work was supported by the Deutsche Forschungsgemeinschaft (DFG) under contracts FA67/25-3 and GRK683 and by the State of Baden-Württemberg, LFSP "Quasiparticles".

APPENDIX A: ASPECTS OF CHIRAL LAGRANGIAN

Using the standard phase conventions for the pseudoscalar meson fields Φ_P and matrices λ_P are given by [23]

$$\begin{aligned}
&\Phi_{\pi^\pm} = -\frac{1}{\sqrt{2}}(\Phi_1 \mp i\Phi_2)\,, \quad \Phi_{K^\pm} = -\frac{1}{\sqrt{2}}(\Phi_4 \mp i\Phi_5)\,,\\
&\Phi_{K^0} = -\frac{1}{\sqrt{2}}(\Phi_6 - i\Phi_7)\,, \quad \Phi_{\bar K^0} = -\frac{1}{\sqrt{2}}(\Phi_6 + i\Phi_7)\,,\\
&\Phi_{\pi^0} = \Phi_3\cos\varepsilon + \Phi_8\sin\varepsilon\,, \quad \Phi_\eta = -\Phi_3\sin\varepsilon + \Phi_8\cos\varepsilon\,,\\
&\\
&\lambda_{\pi^\pm} = -\frac{1}{\sqrt{2}}(\lambda_1 \pm i\lambda_2)\,, \quad \lambda_{K^\pm} = -\frac{1}{\sqrt{2}}(\lambda_4 \pm i\lambda_5)\,,\\
&\lambda_{K^0} = -\frac{1}{\sqrt{2}}(\lambda_6 + i\lambda_7)\,, \quad \lambda_{\bar K^0} = -\frac{1}{\sqrt{2}}(\lambda_6 - i\lambda_7)\,,\\
&\lambda_{\pi^0} = \lambda_3\cos\varepsilon + \lambda_8\sin\varepsilon\,, \quad \lambda_\eta = -\lambda_3\sin\varepsilon + \lambda_8\cos\varepsilon\,.
\end{aligned} \tag{A1}$$

The π^0-η mixing angle ε with

$$\tan 2\varepsilon = \frac{\sqrt{3}}{2}\,\frac{m_d - m_u}{m_s - \hat m}\,, \quad \hat m = \frac{1}{2}\,(m_u + m_d) \tag{A2}$$

is fixed from the diagonalization of the pseudoscalar meson mass term

$$\frac{B}{2}\,\mathrm{Tr}[\hat{\Phi}^2\mathcal{M}] \;=\; \frac{1}{2}\sum_P M_P^2\,\Phi_P^2\,. \tag{A3}$$

The masses of the mesons at leading order are:

$$\begin{aligned}
&M_{\pi^\pm}^2 = 2\hat{m}B\,, \quad M_{K^\pm}^2 = (m_u+m_s)B\,, \quad M_{K^0}^2 = M_{\bar{K}^0}^2 = (m_d+m_s)B\,, \\
&M_{\pi^0}^2 = 2\hat{m}B - \frac{4}{3}(m_s-\hat{m})B\,\frac{\sin^2\varepsilon}{\cos 2\varepsilon}\,, \quad M_\eta^2 = \frac{2}{3}(\hat{m}+2m_s)B + \frac{4}{3}(m_s-\hat{m})B\,\frac{\sin^2\varepsilon}{\cos 2\varepsilon}\,.
\end{aligned} \tag{A4}$$

Finally, with the use of the set $\{\Phi_P, \lambda_P\}$ the linearized Lagrangian (2) can be written as:

$$\begin{aligned}
\mathcal{L}_{\rm eff}(x) &= \bar{\psi}(x)\,[\,i\not{\partial} - S(r) - \gamma^0 V(r) - \mathcal{M}\,]\,\psi(x) - \frac{1}{2}\sum_P \Phi_P(x)[\Box + M_P^2]\Phi_P(x) \\
&\quad - \bar{\psi}(x)\,i\gamma^5\,\frac{S(r)}{F}\,\sum_P \Phi_P(x)\,\lambda_P\,\psi(x)
\end{aligned} \tag{A5}$$

where $\Box = \partial_\mu\partial^\mu$.

REFERENCES

[1] J. Gasser, Annals Phys. **136**, 62 (1981).

[2] E. Reya, Rev. Mod. Phys. **46**, 545 (1974).

[3] R. L. Jaffe, Phys. Rev. D **21**, 3215 (1980).

[4] J. Gasser and M. E. Sainio, arXiv:hep-ph/0002283; M. E. Sainio, PiN Newslett. **16**, 138 (2002) [arXiv:hep-ph/0110413].

[5] P. Schweitzer, arXiv:hep-ph/0307336.

[6] J. Gasser, H. Leutwyler and M. E. Sainio, Phys. Lett. B **253**, 252 (1991); Phys. Lett. B **253**, 260 (1991).

[7] R. Koch, Z. Phys. C **15**, 161 (1982).

[8] T. Becher and H. Leutwyler, Eur. Phys. J. C **9**, 643 (1999) [arXiv:hep-ph/9901384].

[9] T. Fuchs, J. Gegelia and S. Scherer, arXiv:hep-ph/0309234.

[10] B. Borasoy, R. Lewis and P. P. Ouimet, Phys. Rev. D **65**, 114023 (2002) [arXiv:hep-ph/0203199].

[11] W. B. Kaufmann and G. E. Hite, Phys. Rev. C **60**, 055204 (1999).

[12] M. G. Olsson, Phys. Lett. B **482**, 50 (2000) [arXiv:hep-ph/0001203].

[13] M. M. Pavan, I. I. Strakovsky, R. L. Workman and R. A. Arndt, PiN Newslett. **16**, 110 (2002) [arXiv:hep-ph/0111066].

[14] J. Stahov, arXiv:hep-ph/0206041.

[15] V. E. Lyubovitskij, T. Gutsche, A. Faessler and E. G. Drukarev, Phys. Rev. D **63**, 054026 (2001) [arXiv:hep-ph/0009341].

[16] V. E. Lyubovitskij, T. Gutsche and A. Faessler, Phys. Rev. C **64**, 065203 (2001) [arXiv:hep-ph/0105043].

[17] K. Pumsa-ard, V. E. Lyubovitskij, T. Gutsche, A. Faessler and S. Cheedket, Phys. Rev. C **68**, 015205 (2003) [arXiv:hep-ph/0304033].

[18] V. E. Lyubovitskij, T. Gutsche, A. Faessler and R. Vinh Mau, Phys. Lett. B **520**, 204 (2001) [arXiv:hep-ph/0108134]; Phys. Rev. C **65**, 025202 (2002) [arXiv:hep-ph/0109213].

[19] F. Simkovic, V. E. Lyubovitskij, T. Gutsche, A. Faessler and S. Kovalenko, Phys. Lett. B **544**, 121 (2002) [arXiv:hep-ph/0112277].

[20] V. E. Lyubovitskij, P. Wang, T. Gutsche and A. Faessler, Phys. Rev. C **66**, 055204 (2002) [arXiv:hep-ph/0207225].

[21] K. Khosonthongkee *et al.*, in preparation.

[22] J. Gasser, M. E. Sainio and A. Svarc, Nucl. Phys. B **307**, 779 (1988).

[23] J. Gasser and H. Leutwyler, Phys. Rept. **87**, 77 (1982); Nucl. Phys. B **250**, 465 (1985).

[24] M. Procura, T. R. Hemmert and W. Weise, arXiv:hep-lat/0309020.

[25] S. J. Dong, J. F. Lagae and K. F. Liu, Phys. Rev. D **54**, 5496 (1996) [arXiv:hep-ph/9602259].

[26] H. C. Kim, A. Blotz, C. Schneider and K. Goeke, Nucl. Phys. A **596**, 415 (1996) [arXiv:hep-ph/9508299].

[27] C. H. Lee, G. E. Brown, D. P. Min and M. Rho, Nucl. Phys. A **585**, 401 (1995) [arXiv:hep-ph/9406311]. [28]

[28] B. Borasoy, Eur. Phys. J. C **8**, 121 (1999) [arXiv:hep-ph/9807453].

[29] C. Curceanu *et al.* [DEAR Collaboration], Nucl. Phys. A **691**, 278 (2001); R. Baldini *et al.* [DEAR collaboration], LNF-95-055-IR

TABLES

TABLE I. Meson-nucleon sigma terms and related quantities

Quantity	Val	π	K	η	Total
$\sigma_{\pi N}$ (MeV)	13.1	39.4	2.1	0.1	54.7
Δ_σ (MeV)	1	12.5	0.3	0.02	13.8
σ^u_{KN} (MeV)	113.8	256.2	44.7	4.5	419.2
σ^d_{KN} (MeV)	56.9	256.2	35.8	4.5	353.4
$\sigma^{(2)}_{KN}$ (MeV)	0	256.2	26.8	4.5	287.5
$\sigma^{I=0}_{KN}$ (MeV)	85.4	256.2	40.2	4.5	386.3
$\sigma^{I=1}_{KN}$ (MeV)	28.4	0	4.5	0	32.9
$\sigma_{\eta N}$ (MeV)	4.4	13.1	69.4	9.4	96.3
$\langle p\|S_u^{PQCM}\|p\rangle$	1.3	2.8	0.2	0.01	4.3
$\langle p\|S_d^{PQCM}\|p\rangle$	0.6	2.8	0.1	0.01	3.5
$\langle p\|S_s^{PQCM}\|p\rangle$	0	0	0.3	0.04	0.34
F_S	0.63	1.41	− 0.05	− 0.01	1.97
D_S	0	− 1.41	0.15	0.01	− 1.25
$\langle r^2\rangle^S_{\pi N}$ (fm^2)	0.10	1.36	0.04	0.002	1.50
$\langle r^2\rangle^{S;\,(u)}_{KN}$ (fm^2)	0.12	1.16	0.10	0.01	1.39
$\langle r^2\rangle^{S;\,(d)}_{KN}$ (fm^2)	0.07	1.37	0.10	0.01	1.55
$\langle r^2\rangle^{S;\,(2)}_{KN}$ (fm^2)	0	1.69	0.09	0.02	1.80
$\langle r^2\rangle^{S;\,I=0}_{KN}$ (fm^2)	0.10	1.25	0.10	0.01	1.46
$\langle r^2\rangle^{S;\,I=1}_{KN}$ (fm^2)	0.37	0	0.13	0	0.50
$\langle r^2\rangle^S_{\eta N}$ (fm^2)	0.02	0.26	0.71	0.10	1.09

FIGURES

Fig.1: Diagrams contributing to the meson-baryon sigma-terms:
tree diagram (1a), meson cloud diagram (1b) and meson exchange diagram (1c).
Insertion of the scalar density operator is depicted by the symbol " $\vee$ ".

Fig.2: Diagrams contributing to the baryon energy shift:
meson cloud (2a) and meson exchange diagram (2b).

Fig.3: Scalar nucleon form factor $\sigma_{\pi N}(Q^2)$: valence quark, meson cloud and total contributions.

Fig.4: Scalar nucleon form factor $\sigma_{\pi N}(Q^2)$ in comparison to other theoretical approaches (our result - solid line, chiral quark soliton model [5]) - dashed line, relativistic baryon chiral perturbation theory [9] - short-dashed line, NJL-soliton model [26] - dotted line and lattice QCD [25] - dash-dotted line).

Fig.5: Scalar nucleon form factor $\sigma^u_{KN}(Q^2)$: valence quark, meson cloud and total contributions.

Fig.6: Scalar nucleon form factor $\sigma^d_{KN}(Q^2)$: valence quark, meson cloud and total contributions.

Fig.7: Scalar nucleon form factor $\sigma^{(2)}_{KN}(Q^2)$: total (meson cloud) contribution.

Fig.8: Scalar nucleon form factor $\sigma^{I=0}_{KN}(Q^2)$: valence quark, meson cloud and total contributions.

Fig.9: Scalar nucleon form factor $\sigma^{I=1}_{KN}(Q^2)$: valence quark, meson cloud and total contributions.

Fig.10: Scalar nucleon form factor $\sigma_{\eta N}(Q^2)$: valence quark, meson cloud and total contributions.

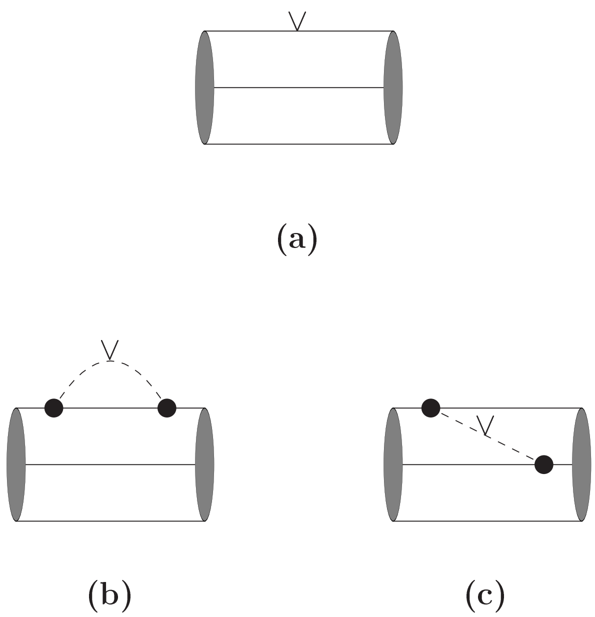

(a)

(b) (c)

Fig.1

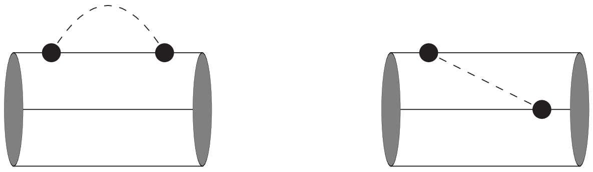

(a) (b)

Fig.2

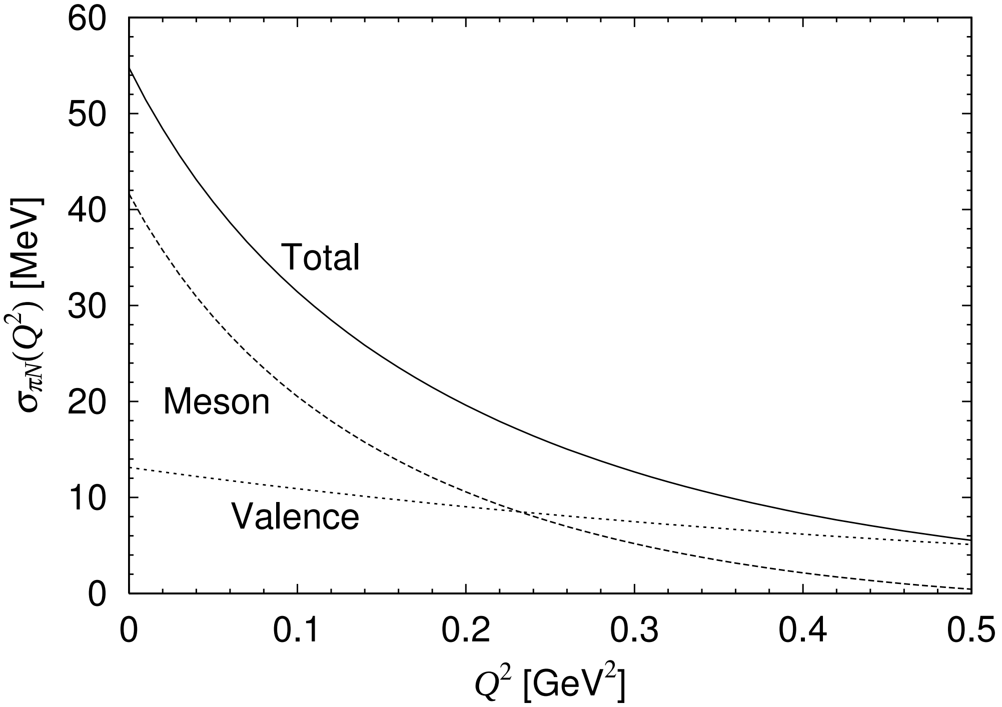
60
50
40
30
20
10
0
0
0.1
0.2
0.3
0.4
0.5
$\sigma_{\pi N}(Q^2)$ [MeV]
Q^2 [GeV^2]
Total
Meson
Valence

Fig.3

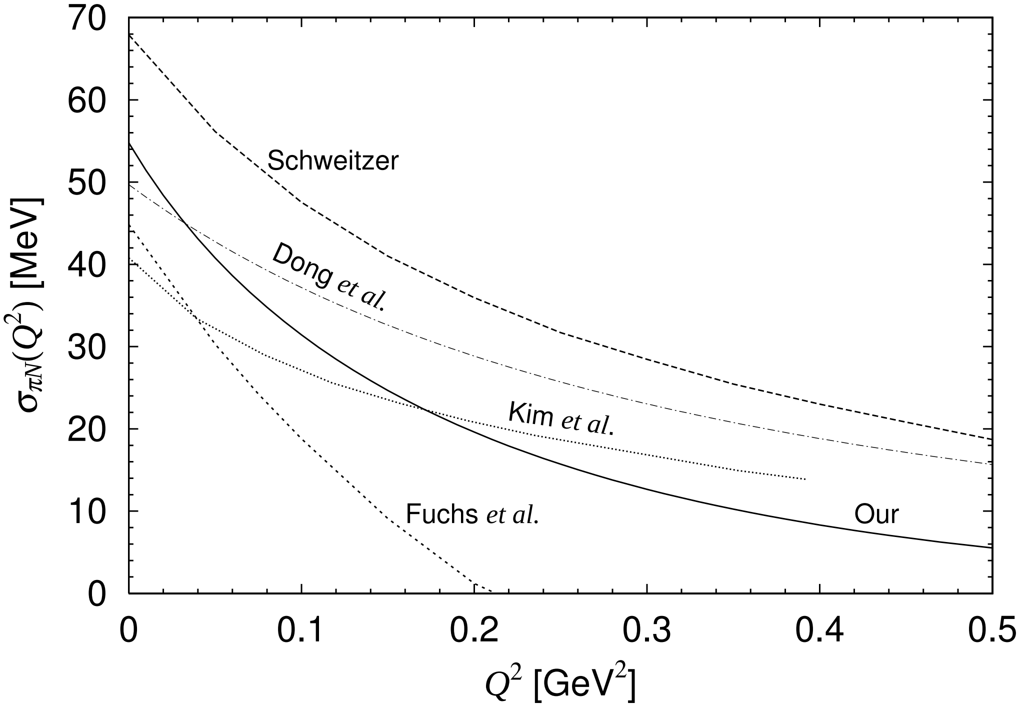

70
60
50
40
30
20
10
0
$\sigma_{\pi N}(Q^2)$ [MeV]
0
0.1
0.2
0.3
0.4
0.5
Q^2 [GeV^2]
Schweitzer
Dong *et al.*
Kim *et al.*
Fuchs *et al.*
Our

Fig.4

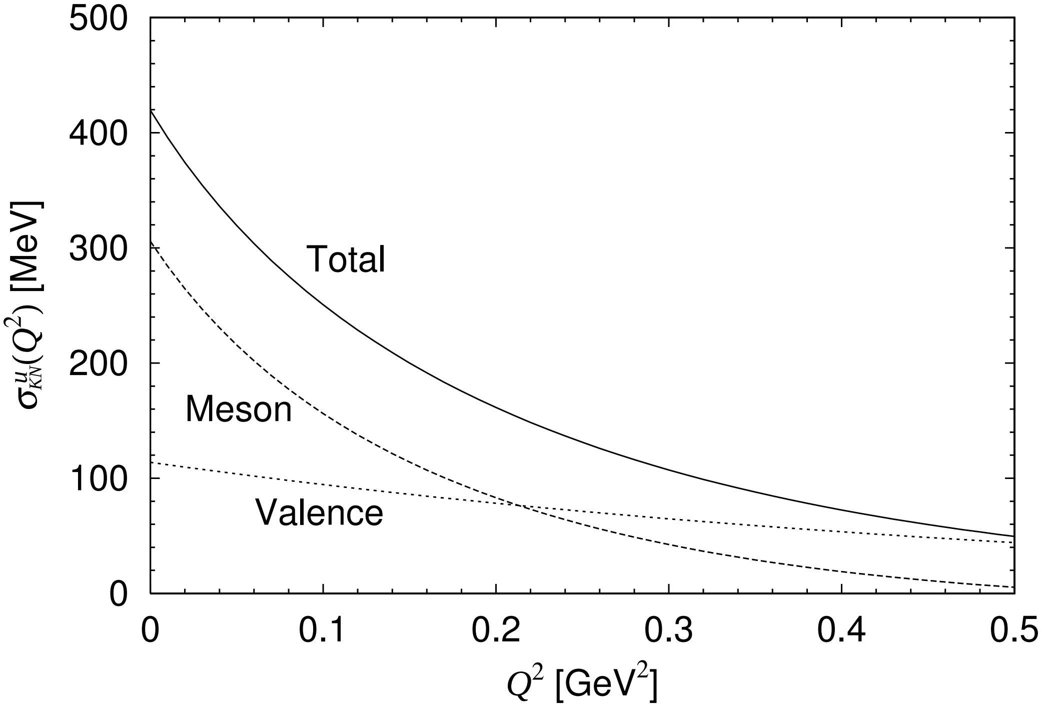

500
400
300
200
100
0
0
0.1
0.2
0.3
0.4
0.5
$\sigma^u_{KN}(Q^2)$ [MeV]
Q^2 [GeV^2]
Total
Meson
Valence

Fig.5

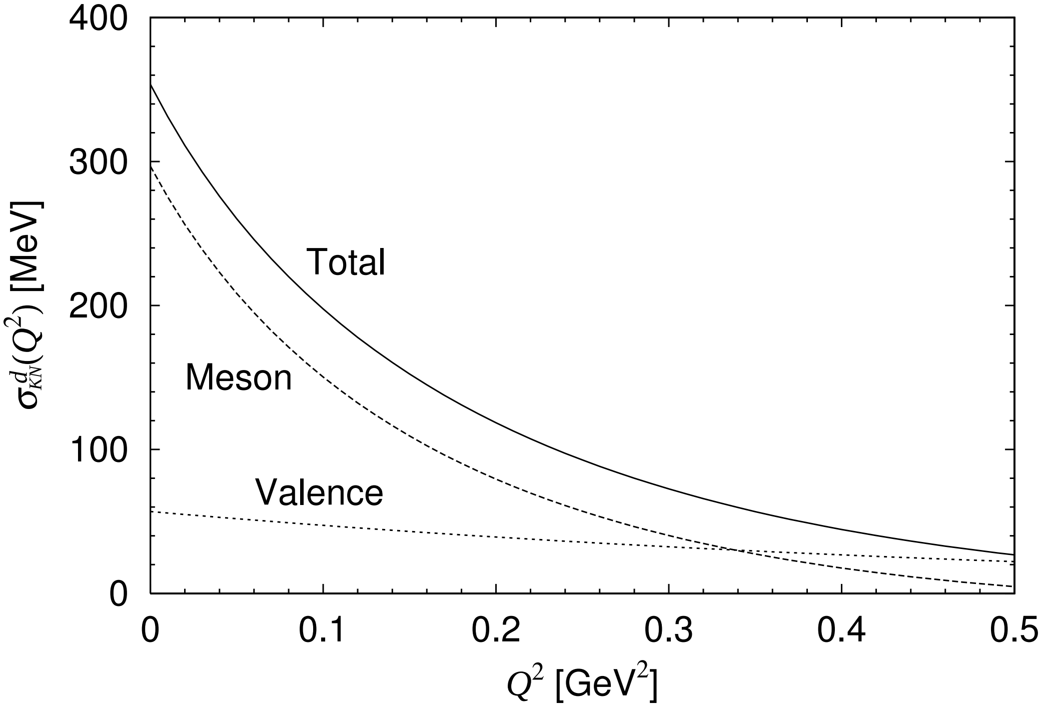

$\sigma^{d}_{KN}(Q^2)$ [MeV]
400
300
200
100
0
0
0.1
0.2
0.3
0.4
0.5
Q^2 [GeV^2]
Total
Meson
Valence

Fig.6

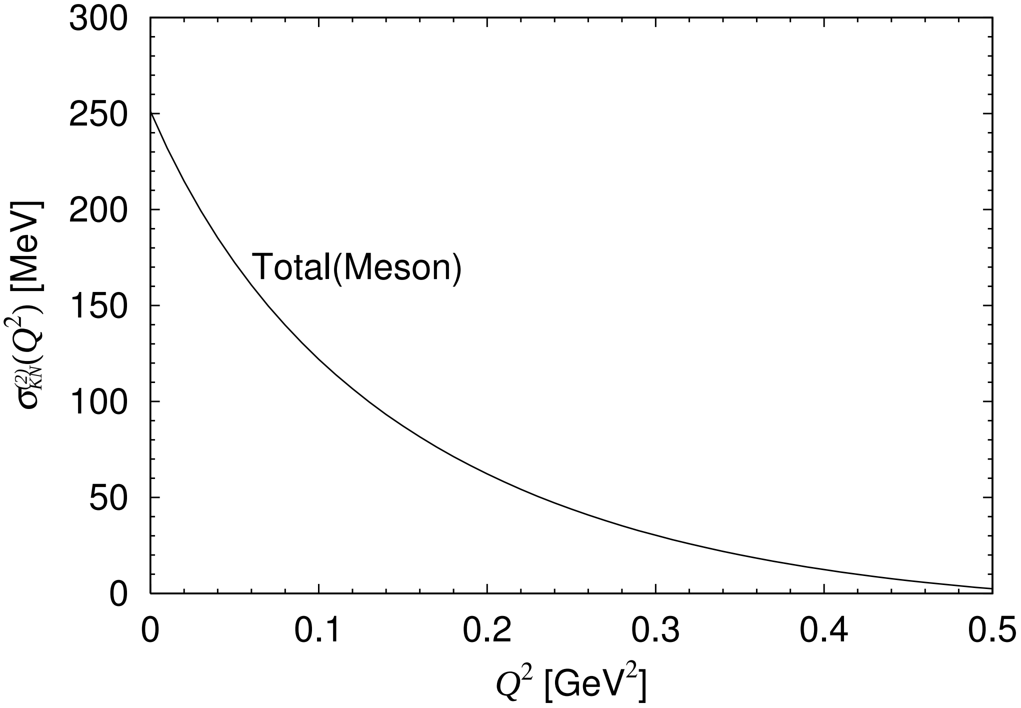
300
250
200
150
100
50
0
0
0.1
0.2
0.3
0.4
0.5
$\sigma^{(2)}_{KN}(Q^2)$ [MeV]
Q^2 [GeV^2]
Total(Meson)

Fig.7

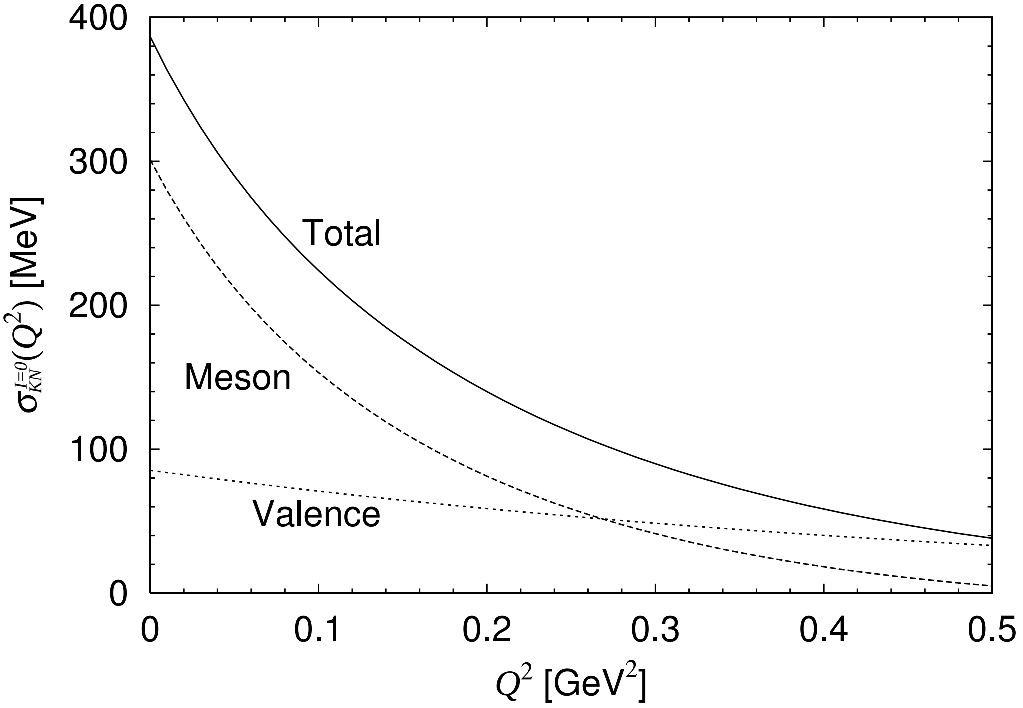

$\sigma_{KN}^{I=0}(Q^2)$ [MeV]
400
300
200
100
0
0
0.1
0.2
0.3
0.4
0.5
Q^2 [GeV^2]
Total
Meson
Valence

Fig.8

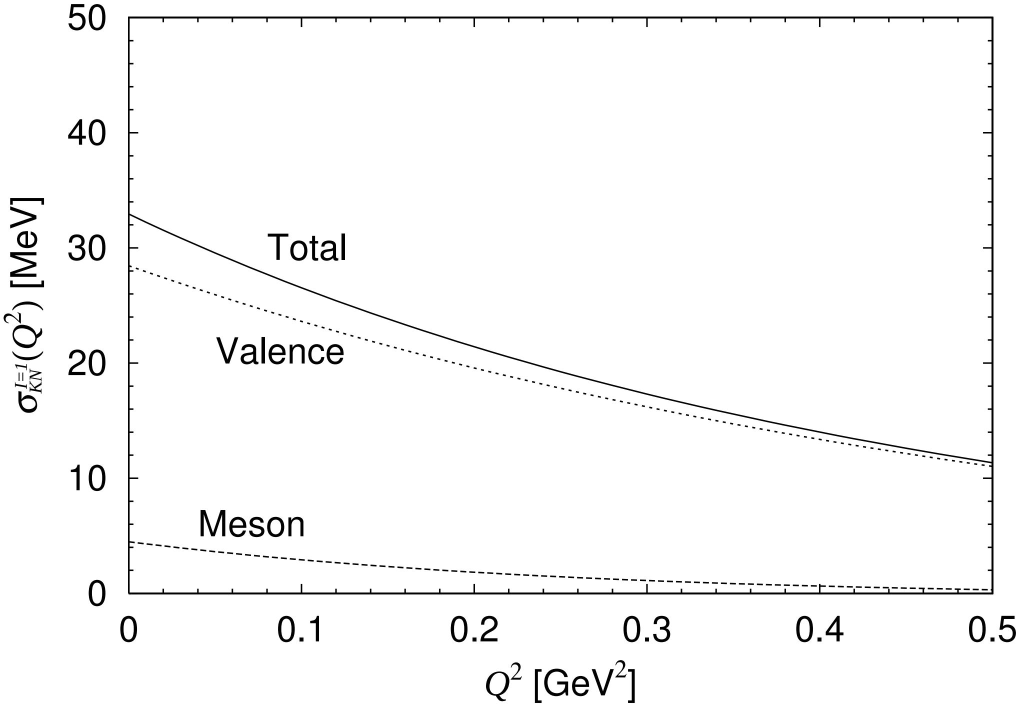

$\sigma_{KN}^{I=1}(Q^2)$ [MeV]
Q^2 [GeV^2]
0
10
20
30
40
50
0
0.1
0.2
0.3
0.4
0.5
Total
Valence
Meson

Fig.9

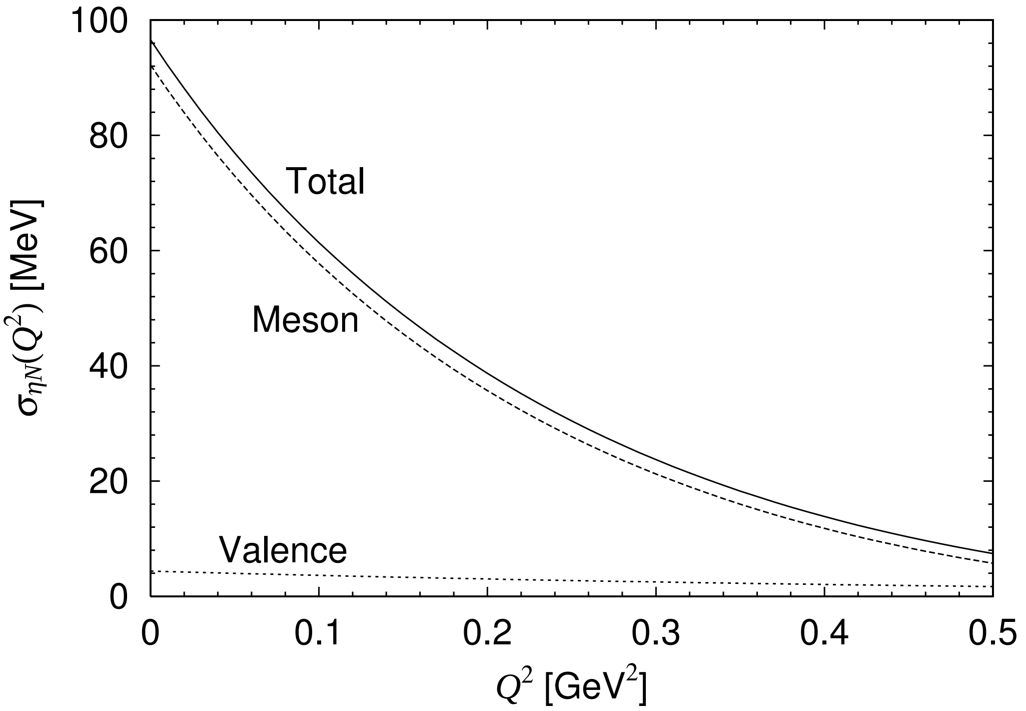

100
80
60
40
20
0
0
0.1
0.2
0.3
0.4
0.5
$\sigma_{\eta N}(Q^2)$ [MeV]
Q^2 [GeV^2]
Total
Meson
Valence

Fig.10